Desalination and Water Treatment
www.deswater.com
doi: 10.1080/19443994.2014.883334

54 (2015) 374–381
April

Taylor & Francis
Taylor & Francis Group

Photocatalytic degradation of Rhodamine 6G using ZnO-montmorillonite nanocomposite: a kinetic approach

Sandip P. Patil[a], V.S. Shrivastava[a], G.H. Sonawane[b,*]

[a]*Nano-chemistry Research Laboratory, G. T. Patil College, Nandurbar 425 412 (M.S.), India*
[b]*Department of Chemistry, Kisan Arts, Commerce and Science College, Parola 425 111 (M.S.), India*
Tel./Fax: +912597222441; email: drgunvantsonawane@gmail.com

Received 15 November 2013; Accepted 5 January 2014

ABSTRACT

Montmorillonite clay was incorporated with ZnO to get ZnO-montmorillonite nanocomposite. This nanocomposite was successfully used for removal of Rhodamine 6G by photocatalytic degradation and adsorption. The influence of contact time, initial dye concentration, pH and catalyst dose has been determined. Contact time of 80 min and pH 3 was optimized for photocatalytic degradation of Rhodamine 6G. Kinetic parameters like pseudo-first-order, pseudo-second-order, Elovich and intraparticle diffusion model were determined. Pseudo-second-order kinetics could describe the adsorption kinetics well with $r^2 > 0.997$ for 20–150 mg/L dye concentrations. Adsorption isotherms like Langmuir and Freundlich isotherm are used to describe the adsorption of dye. The monolayer capacity was observed to be 200 mg/g. Freundlich adsorption isotherm was found to fit better than Langmuir isotherm. Removal of Rhodamine 6G could be increased by combine effect of photocatalytic degradation and adsorption by nanocomposite.

Keywords: Photocatalyst; Rhodamine 6G; Nanocomposite; Adsorption; Isotherm

1. Introduction

The textile dyeing and printing industries produce large volume of wastewater. This is responsible for water pollution, as it contains large amount of consumed dyes. It is found that nearly 1–15% dye is lost and released in wastewater from textile industry [1]. There are several methods for treatment of wastewater from textile dye industry in order to remove harmful materials or contaminants. These materials include organics as well as inorganic pollutants, which are present in large quantities in wastewater discharged into the ecosystem. Sometimes these methods are insufficient as some of the dyes are quite stable. Adsorption using activated carbon has been found to be an efficient method due to its high adsorption capacity. But high regeneration cost of activated carbon leads to search other alternatives. Some of the methods include use of biosorbents like wheat bran [2], groundnut shell [3], rice husk [4], peanut husk [5] and maize cob [6] for the removal of textile dyes. Clay minerals are also used due to their adsorption–desorption properties.

One of the most promising techniques employed for eliminating organic pollutants mainly focuses on their oxidative mineralization by heterogeneous photocatalysis involving advanced oxidation processes [7–11]. The higher mobility of the photogenerated

*Corresponding author.

carriers (including holes and electrons) and deeper VB of a semiconductor can enhance its photocatalytic oxidative activity leading to the decomposition of the organics [12].

ZnO generates more negative potential of electron, so it is effectively used for photocatalytic degradation. Natural clay being inexpensive and easily available is used for adsorption of organics from wastewater. Clays are also incorporated with photocatalysts to form clay composites. Photocatalytic reactivity of such composites enhanced due to the basal space and cation exchange capacity [7]. Such nanocomposite shows better catalytic efficiency when compared with nanoparticles alone.

In present study, ZnO-montmorillonite nanocomposite was synthesized, and kinetics of photocatalytic degradation and adsorption of Rhodamine 6G using ZnO-montmorillonite were investigated.

2. Materials and methods

2.1. Preparation of ZnO-montmorillonite nanocomposite

ZnO-montmorillonite was prepared by adding the aqueous mixture of zinc chloride and sodium hydroxide solutions (1:15) into the aqueous suspension of Na-montmorillonite with continuous stirring at 70°C and the mixture was allowed to react for 24 h. The resulting solids were separated by centrifugation, washed several times with deionized water and dried at 50°C for three days [13].

2.2. Preparation of Rhodamine 6G solution

The stock solution of Rhodamine 6G was prepared in distilled water (500 mg/L). The experimental solutions of required concentration were prepared by diluting the stock solution with distilled water. All other chemicals NaOH and $ZnCl_2$ were of analytical grade. The molecular structure of Rhodamine 6G is shown in Fig. 1.

2.3. Adsorption study

The photocatalytic degradation of Rhodamine 6G was carried out in photocatalytic reactor, having 400 W mercury lamp. The energy of photon for mercury light was 4.53×10^{-19} J. The cooling water jacket was set-up inside the reactor to maintain the temperature. The dye solution was stirred with magnetic stirrer to maintain thorough mixing throughout the experiment. Different nanocomposite dose was added in 50 ml dye solution and irradiated with mercury lamp. At regular time intervals, suitable amount of sample was withdrawn and centrifuged. Then changes in dye concentration were determined by UV-visible double beam spectrophotometer (Systronics model-2203) at λ_{max} 530 nm. The removal percentage of Rhodamine 6G and the amount of Rhodamine 6G adsorbed were calculated using Eqs. (1) and (2):

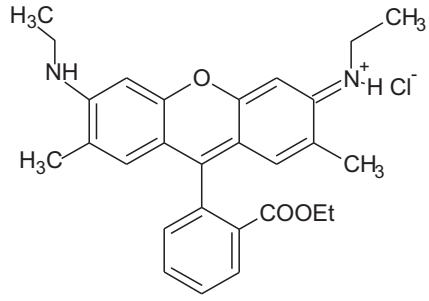

Fig. 1. Molecular structure of the Rhodamine 6G.

$$\text{Removal percentage} = \left(\frac{C_0 - C_t}{C_0}\right) \times 100 \quad (1)$$

$$q_t = \frac{(C_0 - C_t)V}{W} \quad (2)$$

where C_0 (mg/L) is the initial dye concentration; C_t (mg/L) is the concentration of Rhodamine 6G at time t; q_t (mg/g) is the adsorption capacity; V (L) is the initial volume of dye solution and W (g) is the amount of adsorbent.

3. Results and discussion

3.1. Scanning electron microscopy (SEM) analysis

SEM is widely used to study the morphological characteristics of adsorbent. The ZnO-montmorillonite nanocomposite was analysed by SEM before and after adsorption of Rhodamine 6G. Fig. 2(a) and (b) shows the SEM micrographs of ZnO-montmorillonite and ZnO-montmorillonite dyed with Rhodamine 6G. From SEM micrographs of ZnO-montmorillonite it was observed that it has heterogeneous surface, micropores and mesopores.

3.2. X-ray diffraction (XRD) analysis

The XRD diagram of ZnO-montmorillonite is shown in Fig. 3. It shows main peak at 2θ of 25.7° and secondary peaks at 2θ of 34° and 60.9°, respectively. The high intensity of peaks indicates the highly crystalline nature of the ZnO-montmorillonite.

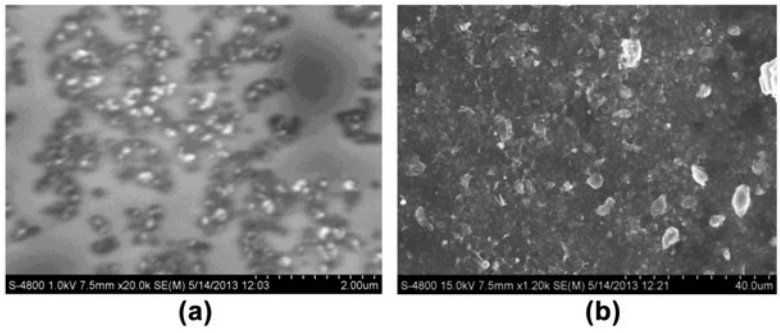

Fig. 2. The SEM micrographs of ZnO-montmorillonite and ZnO-montmorillonite dyed by Rhodamine 6G.

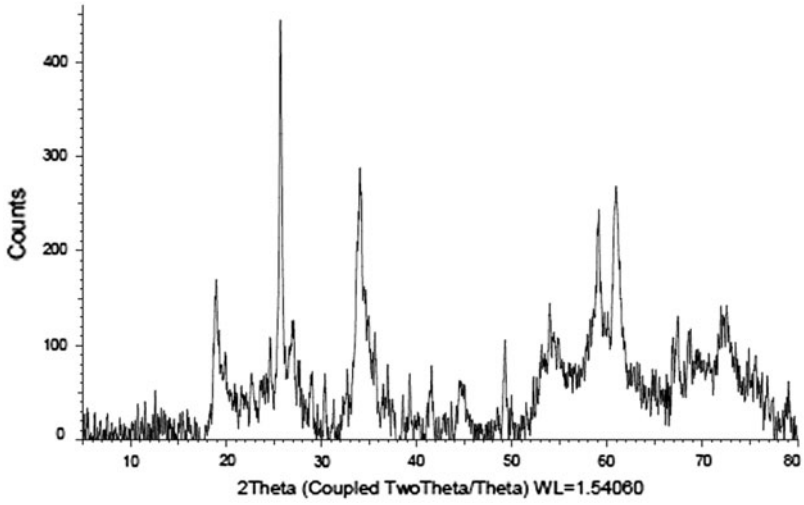

Fig. 3. XRD diagram of ZnO-montmorillonite.

3.3. Effect of contact time

The effect of contact time and initial dye concentration on percentage removal of Rhodamine 6G by ZnO-montmorillonite is shown in Figs. 4 and 5. It was observed that the rate of dye removal is faster for first 40 min, then thereafter it increases and finally attains the equilibrium. As contact time increases percentage removal also increases and attains equilibrium at 80 min and after that it remains constant. The percentage removal at equilibrium decreases from 97.8 to 90.3% as dye concentration was increased from 20 to 150 mg/L for 1 g/L catalyst dose. The amount of dye adsorbed q_t (mg/g) increases from 19.55 to 136.88 mg/g as shown in Fig. 5.

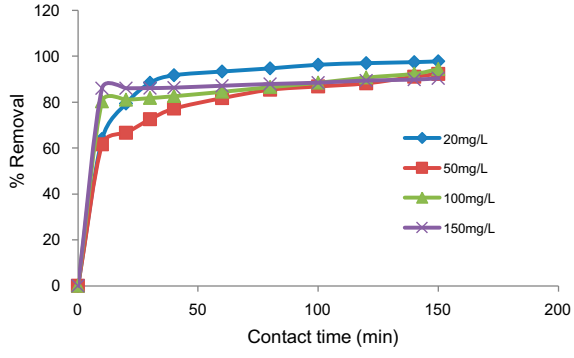

Fig. 4. Effect of contact time and initial concentration of Rhodamine 6G on percentage removal; pH 3, adsorbent dose 1 g/L.

3.4. Effect of pH

The pH of dye solution has significant effect on photocatalytic degradation of dye. The effect of pH on photocatalytic degradation of Rhodamine 6G was studied from pH 2–9 at initial concentration 20 mg/L with catalyst dose 1 g/L. It was observed that percentage removal was 97.9% at pH 2 and 98.1% at pH 3. At

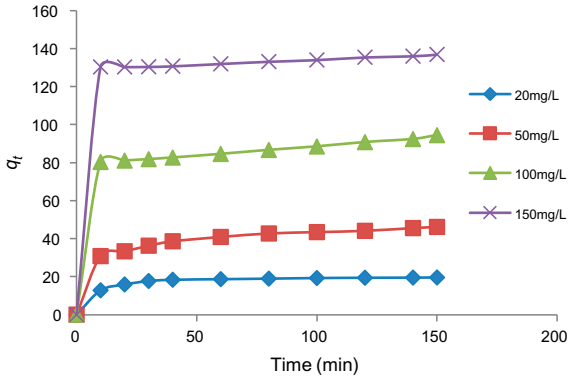

Fig. 5. Amount of dye adsorbed q_t (mg/g) with time for different initial dye concentration; pH 3, adsorbent dose 1 g/L.

pH 3, the percentage removal was higher, then thereafter it decreases up to 91.4% at pH 9.

3.5. Effect of catalyst dose

The effect of photocatalyst dose was studied on dye removal keeping other experimental conditions constant. The percentage removal of Rhodamine 6G by ZnO-montmorillonite at different catalyst doses 0.1–2.4 g/L for 20–80 mg/L of dye concentration was studied. Fig. 6 shows the effect of catalyst dose on amount of dye adsorption. The amount of dye adsorbed (q_t) increases from 106.9 to 603.8 mg/g when dye concentration increases from 20 to 80 mg/L and catalyst dose is 0.1 g/L. As adsorbent dose increases from 0.1 to 2.4 g/L, the amount of dye adsorbed per unit mass of adsorbent (mg/g) decreases from 603.8 to 32.5 mg/g at dye concentration 80 mg/L, while percentage removal increases from 75.5 to 97.5%. The results show that as adsorbent mass increases, the

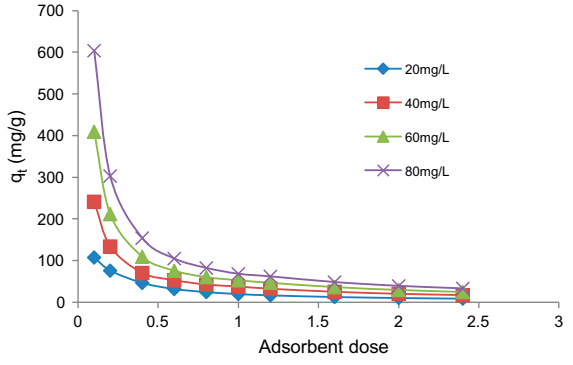

Fig. 6. Amount of dye adsorbed q_t (mg/g) with adsorbent dose (g/L) for different initial concentrations, contact time 150 min, pH 3.

percentage of dye adsorbed also increases but amount adsorbed per unit mass of adsorbent decreases considerably.

3.6. Adsorption kinetics

The adsorption kinetics gives the idea about mechanism of adsorption, from which efficiency of process is estimated. The kinetics of adsorption of Rhodamine 6G on ZnO-montmorillonite was studied with the help of pseudo-first-order, pseudo-second-order, Elovich and intraparticle diffusion models.

3.6.1. The pseudo-first-order model

A linear form of pseudo-first-order was described by Lagergren [14] is as follows (Eq. 3):

$$\log(q_e - q_t) = \log q_e - \frac{K_1 t}{2.303} \tag{3}$$

where q_e and q_t are the amount of dye adsorbed (mg/g) on ZnO-montmorillonite at equilibrium and at time t, respectively. K_1 is the rate constant of pseudo-first-order adsorption (min^{-1}). A plot of log ($q_e - q_t$) vs t gives the value of rate constant. The linear relationship of the plot for 20, 50, 100 and 150 mg/L dye concentrations indicates validity of equation. The calculated K_1 and co-relation coefficient r^2 values are shown in Table 1. Even though co-relation coefficient r^2 for the plots are ≥ 0.912, the calculated q_e values from first-order-kinetics plots were too small when compared with the experimental q_e values (Table 1). This shows that pseudo-first-order model is non-applicable to predict the adsorption kinetics of Rhodamine 6G on ZnO-montmorillonite.

3.6.2. The pseudo-second-order model

The pseudo-second-order kinetics model is expressed as [5,15] follows (Eq. 4):

$$\frac{t}{q_t} = \frac{1}{K_2 q_e^2} + \frac{t}{q_e} \text{ and } h = K_2 q_e^2 \tag{4}$$

where K_2 is rate constant for second-order adsorption (g mg^{-1} min^{-1}), h is the initial rate (mg g^{-1} min). K_2 and q_e are determined from slope and intercept of plot of t/q_t vs t (Fig. 7). The linear plot with co-relation coefficient (r^2) 0.997–0.999 (Table 1) shows a good agreement of experimental data for different initial dye concentrations 20, 50, 100 and 150 mg/L.

Table 1
Comparison of adsorption rate constants, calculated and experimental q_e values for different initial dye concentrations and adsorbent dose for different kinetic models

		Pseudo-first-order			
Adsorbent (g/L)	Dye concentration (mg/L)	q_e (exp) (mg/g)	K_1 (min^{-1})	q_e (cal) (mg/g)	r^2
1	20	19.547	0.0299	6.095	0.968
	50	46.126	0.0184	19.679	0.957
	100	94.411	0.0115	19.454	0.930
	150	136.881	0.0115	10.046	0.912
3	50	16.565	0.0161	0.736	0.962
	100	33.093	0.0207	2.858	0.971
	150	49.733	0.0253	4.036	0.989
		Pseudo-second-order			
		$K_2 \times 10^{-3}$(g/mg min)	q_e (exp) (mg/g)	h	r^2
1	20	9.72	20.41	4.05	0.999
	50	2.12	50.00	5.32	0.998
	100	1.89	100.00	18.87	0.997
	150	4.45	142.86	90.91	0.999
3	50	76.56	16.67	21.28	0.999
	100	21.43	33.33	23.81	0.999
	150	17.39	50.00	43.48	0.999

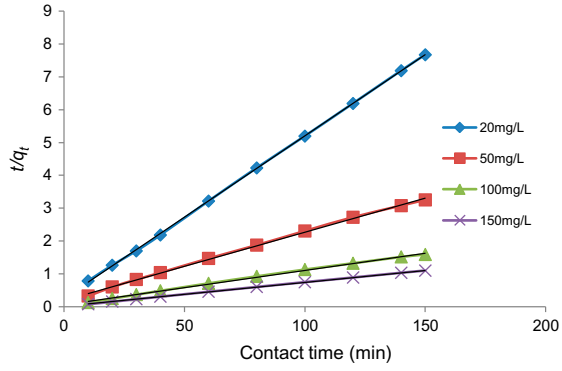

Fig. 7. Second-order-kinetics plots for the removal of Rhodamine 6G at different initial dye concentrations; adsorbent dose 1 g/L, pH 3.

The calculated q_e value is in good agreement with the experimental q_e values shows that adsorption belongs to the second-order-kinetics. It has been observed that rate constants for second-order model decreased with increase in initial dye concentration and increases with increase in adsorbent dose (Table 1).

3.6.3. The Elovich equation

The simplified Elovich equation [4] is as follows (Eq. 5):

$$q_t = \frac{1}{\beta}\ln(\alpha\beta) + \frac{1}{\beta}\ln t \tag{5}$$

where α is the initial adsorption rate (mg g^{-1} min^{-1}), β is the desorption constant (g/mg). These are calculated from intercept and slope of the linear plot of q_t vs ln t. The value of β decreases from 1.5974 to 0.3166 g/mg for 3 g/L of adsorbent dose. The β value increases from 0.0751 to 1.5974 g/mg as adsorbent dose increased from 1 to 3 g/L for 50 mg/L of dye concentration (Table 2).

3.6.4. The intraparticle diffusion model

In a solid–liquid adsorption, adsorption depends on film diffusion initially and thereafter on intraparticle diffusion [16,17]. According to Weber and Morris [18], if intraparticle diffusion is the rate-controlling factor then amount of adsorbate adsorbed varies with the square root of time. Weber–Morris plot is given by Eq. (6):

$$q_t = K_p t^{1/2} + C \tag{6}$$

where K_p is intraparticle diffusion rate constant (mg/g/$min^{0.5}$). The plot of q_t vs $t^{1/2}$ is linear indicates occurrence of intraparticle diffusion as shown in Fig. 8. The K_p has values 0.051–0.282 mg/g/$min^{0.5}$ for 50, 100 and 150 mg/L dye concentrations and 3 g/L photocatalyst dose (Table 2).

Table 2
Adsorption kinetics parameters of Rhodamine 6G onto ZnO-montmorillonite for Elovich and intra-particle diffusion models

Adsorbent (g/L)	Dye concentration (mg/L)	Elovich model			Intraparticle diffusion	
		β (g/mg)	α (mg/g min)	r^2	K_p (mg/g/min$^{0.5}$)	r^2
1	20	0.1967	0.31×10^2	0.870	0.370	0.801
	50	0.0751	0.47×10^2	0.992	1.496	0.966
	100	0.0845	3.03×10^3	0.857	1.645	0.943
	150	0.1716	8.12×10^9	0.815	0.854	0.944
3	50	1.5974	2.19×10^{10}	0.920	0.051	0.991
	100	0.4850	7.95×10^5	0.983	0.209	0.929
	150	0.3166	3.82×10^6	0.955	0.282	0.909

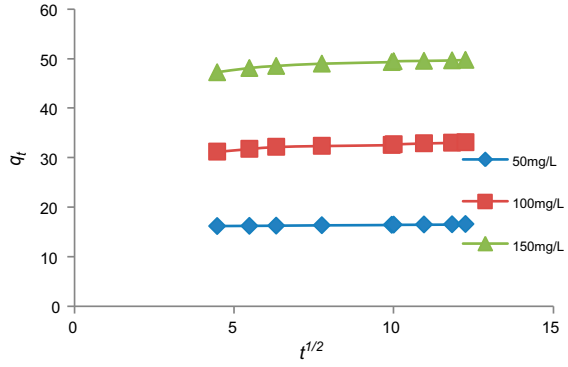

Fig. 8. Weber–Morris plot for adsorption of Rhodamine 6G by ZnO-montmorillonite.

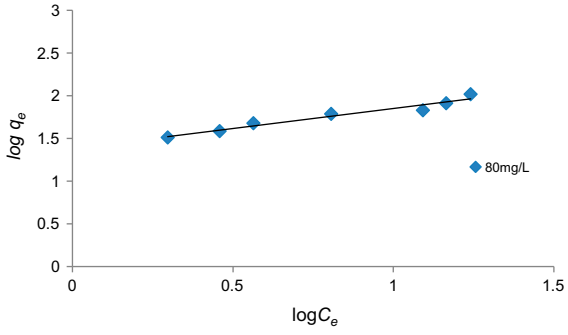

Fig. 9. Freundlich plot for adsorption of Rhodamine 6G by ZnO-montmorillonite.

3.7. Adsorption isotherms

The relationship between amount of adsorbate and adsorbent surface is represented by adsorption isotherms. Adsorption equilibrium is established when adsorbate phase is in contact with adsorbent for sufficient time. Over a wide variety of equilibrium adsorption isotherms, Langmuir and Freundlich isotherms are the most common isotherms.

3.7.1. Freundlich isotherm model

Freundlich isotherm describes the non-ideal, reversible adsorption with heterogeneous system and applied to multilayer adsorption. Freundlich isotherm [2,19] is given by Eq. (7):

$$\log q_e = \log K_F + \frac{1}{n}\log C_e \tag{7}$$

where q_e is amount of dye adsorbed per unit mass of adsorbent (mg/g), C_e is equilibrium concentration of dye, K_F is Freundlich isotherm constant (mg/g) (L/g)^n related to adsorption capacity, $1/n$ is a measure of adsorption density. Linearity of the plot of log q_e vs log C_e indicates that adsorption also follows Freundlich isotherm as shown in Fig. 9. When slope ($1/n$) is closer to zero, adsorption becomes more heterogeneous. $1/n$ less than unity indicates chemisorptions while above unity indicates co-operative adsorption [20]. The values of $1/n$ between 0.432 and 0.561 for 20–80 mg/L of Rhodamine 6G indicate that it is chemisorption. The calculated K_F and $1/n$ values are presented in Table 3.

3.7.2. Langmuir isotherm model

Langmuir assumes that the homogeneous monolayer adsorption occurs at the finite number of identical and equivalent sites with no interaction between adsorbed molecules. The linear form of Langmuir isotherm [3,21] is as follows (Eq. 8):

$$\frac{C_e}{q_e} = \frac{1}{ab} + \frac{C_e}{a} \tag{8}$$

Table 3
Freundlich and Langmuir isotherm constants for adsorption of Rhodamine 6G on ZnO-montmorillonite for different dye concentration and adsorbent dose of 0.1–2.4 g/L at pH 3, contact time 150 min

	Freundlich coefficient				Langmuir coefficient			
Dye concentration (mg/L)	K_F (L/g)	n	$1/n$	r^2	a (mg/g)	b (g/L)	R_L	r^2
20	30.974	1.7825	0.5610	0.971	200.00	0.1515	0.2481	0.946
40	21.330	2.3148	0.4320	0.944	80.33	0.2857	0.0805	0.915
60	20.845	2.1786	0.4590	0.948	90.91	0.2157	0.0717	0.957
80	24.155	2.1322	0.4689	0.952	100.00	0.2381	0.0499	0.973

where a denotes monolayer coverage capacity (mg/g), b is Langmuir isotherm constant (L/mg). Linear nature of plot C_e/q_e vs C_e shows that adsorption follows Langmuir isotherm (Fig. 10). Calculated a and b values are presented in Table 3. The Langmuir adsorption suggests the monolayer coverage of dye on ZnO-montmorillonite. According to Webber and Chakkravorti, Langmuir isotherm can be expressed by dimensionless factor which is also known as separation factor R_L. It is expressed [22] as follows (Eq. 9):

$$R_L = \frac{1}{1 + bC_i} \tag{9}$$

where b is the Langmuir constant and C_i is the initial dye concentration (mg/L). The R_L value indicates adsorption nature. When $R_L > 1$ adsorption is unfavourable, $R_L = 1$ adsorption is linear, $1 > R_L > 0$ adsorption is favourable and $R_L = 0$ adsorption is irreversible. In the present study, the lower R_L value ($R_L < 1$) represents adsorption is favourable.

The co-relation coefficient r^2 values for Langmuir and Freundlich isotherms are shown in Table 3. Both the isotherms found to fit well to experimental data with Freundlich having higher r^2 values than Langmuir isotherm. Thus Freundlich adsorption is most appropriate for adsorption of Rhodamine 6G on ZnO-montmorillonite.

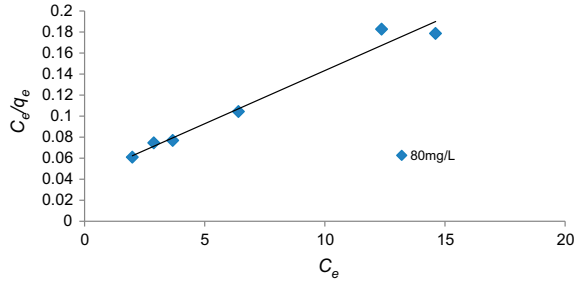

Fig. 10. Langmuir plot for adsorption of Rhodamine 6G by ZnO-montmorillonite.

4. Conclusion

The experimental results show that ZnO-montmorillonite was found to be promising for removal of Rhodamine 6G from aqueous solution. q_e values for Rhodamine 6G adsorption were dependent on contact time, pH, dye concentration and adsorbent dose. The lower pH 3 favours removal of dye. The amount of dye adsorbed (mg/g) was found to be increase with increase in contact time and initial dye concentration and to decrease with increase in catalyst dose. The adsorption kinetics was found to confirm pseudo-second-order kinetics with higher co-relation coefficient. Adsorption isotherms were described by Langmuir isotherm and Freundlich isotherm models. Freundlich isotherm model was found to fit experimental data due to higher $1/n$ and K_F values. Dimensionless factor (R_L) showed that ZnO-montmorillonite can be effectively used for removal of Rhodamine 6G dye from aqueous solution.

Acknowledgements

The authors are gratefully acknowledged to Central Instrumentation Centre, University Institute of Chemical Technology, NMU, Jalgaon for SEM and XRD analysis. Authors are also thankful to Principal, GTP College Nandurbar and Principal, Kisan College, Parola for providing necessary laboratory facilities.

References

[1] N. Barka, A. Assabbane, A. Nounah, L. Laanab, Y.A. Ichou, Removal of textile dyes from aqueous solutions by natural phosphate as a new adsorbent, Desalination 235 (2009) 264–275.
[2] M.T. Sulak, H.C. Yatmaz, Removal of textile dyes from aqueous solutions with eco-friendly biosorbent, Desalin. Water Treat. 37 (2012) 169–177.
[3] G.H. Sonawane, V.S. Shrivastava, Removal of hazardous dye from synthetic textile dyeing and printing effluents by *Archis hypogaea L.* shell: A low cost agro waste material, Desalin. Water Treat. 29 (2011) 29–38.
[4] M.C. Shih, Kinetics of the batch adsorption of Methylene blue from aqueous solutions onto rice husk: Effect

of acid-modified process and dye concentration, Desalin. Water Treat. 37 (2012) 200–214.
[5] Z. Hu, N. Wang, J. Tan, J. Chen, W. Zhong, Kinetic and equilibrium of cefradine adsorption onto peanut husk, Desalin. Water Treat. 37 (2012) 160–168.
[6] G.H. Sonawane, V.S. Shrivastava, Kinetics of decolourization of malachite green from aqueous medium by maize cob (Zea maize): An agricultural solid waste, Desalination 251 (2009) 1–12.
[7] S. Meshram, R. Limaye, S. Ghodke, S. Nigam, S. Sonawane, R. Chikate, Continuous flow photocatalytic reactor using ZnO–bentonite nanocomposite for degradation of phenol, Chem. Eng. J. 172 (2011) 1008–1015.
[8] G. Centi, S. Perathoner, One-step H_2O_2 and phenol syntheses: Examples of challenges for new sustainable selective oxidation processes, Catal. Today 143(1–2) (2009) 145–150.
[9] A. Matilainen, M. Sillanpää, Removal of natural organic matter from drinking water by advanced oxidation processes, Chemosphere 80(4) (2010) 351–365.
[10] G. Palmisano, V. Augugliaro, M. Pagliaro, L. Palmisano, Photocatalysis: A promising route for 21st century organic chemistry, Chem. Commun. (2007) 3425–3437.
[11] K. Demeestere, J. Dewulf, H. Van Langenhove, Heterogeneous photocatalysis as an advanced oxidation process for the abatement of chlorinated, monocyclic aromatic and sulfurous volatile organic compounds in air: State of the art, Crit. Rev. Env. Sci. Technol. 37 (2007) 489–538.
[12] J. Sato, H. Kobayashi, K. Ikarashi, N. Saito, H. Nishiyama, Y. Inoue, Photocatalytic activity for water decomposition of RuO_2-dispersed Zn_2GeO_4 with d^{10} configuration, J. Phy. Chem. B 108 (2004) 4369–4375.
[13] N. Khaorapapong, N. Khumchoo, M. Ogawa, Preparation of zinc oxide–montmorillonite hybrids, Mater. Lett. 65 (2011) 657–660.
[14] N.K. Amin, Removal of direct blue-106 dye from aqueous solution using new activated carbons developed from pomegranate peel: Adsorption equilibrium and kinetics, J. Hazard. Mater. 165 (2009) 52–62.
[15] M.A.M. Salleh, D.K. Mahmoud, W.A.W.A. Karim, A. Idris, Cationic and anionic dye adsorption by agricultural solid wastes: A comprehensive review, Desalination 280 (2011) 1–13.
[16] B.H. Hameed, M.I. El-Khaiary, Sorption kinetics and isotherm studies of a cationic dye using agricultural waste: Broad bean peels, J. Hazard. Mater. 154 (2008) 639–648.
[17] M. Alkan, M. Doğan, Y. Turhan, Ö. Demirbaş, P. Turan, Adsorption kinetics and mechanism of maxilon blue 5G dye on sepiolite from aqueous solutions, Chem. Eng. J. 139 (2008) 213–223.
[18] W.J. Weber, J.C. Morris, Kinetics of adsorption on carbon from solution, J. Sanitary Eng. Div. Proc. Am. Soc. Civil. Eng. 89 (1963) 31–59.
[19] K.Y. Foo, B.H. Hameed, Insights into the modeling of adsorption isotherm systems, Chem. Eng. J. 156 (2010) 2–10.
[20] F. Haghseresht, G. Lu, Adsorption characteristics of phenolic compounds onto coal-reject-derived adsorbents, Energ. Fuels 12 (1998) 1100–1107.
[21] C. Kannan, K. Muthuraja, M.R. Devi, Hazardous dyes removal from aqueous solution over mesoporous aluminophosphate with textural porosity by adsorption, J. Hazard. Mater. 244–245 (2013) 10–20.
[22] S.D. Khattri, M.K. Singh, Removal of malachite green from dye wastewater using neem sawdust by adsorption, J. Hazard. Mater. 167 (2009) 1089–1094.